ORGANIC LETTERS

2011
Vol. 13, No. 14
3652–3655

Perylene Anhydride Fused Porphyrins as Near-Infrared Sensitizers for Dye-Sensitized Solar Cells

Chongjun Jiao,[†] Ningning Zu,[‡] Kuo-Wei Huang,[§] Peng Wang,*[,‡] and Jishan Wu*[,†,∥]

*Department of Chemistry, National University of Singapore, 3 Science Drive 3, Singapore, 117543, State Key Laboratory of Polymer Physics and Chemistry, Changchun Institute of Applied Chemistry, Chinese Academy of Sciences, Changchun, 130022, P. R. China, KAUST Catalysis Center and Division of Chemical and Life Sciences and Engineering, 4700 King Abdullah University of Science and Technology, Thuwal 23955-6900, Kingdom of Saudi Arabia, and Institute of Materials Research and Engineering, A*Star, 3 Research Link, Singapore, 117602*

peng.wang@ciac.jl.cn; chmwuj@nus.edu.sg

Received May 14, 2011

ABSTRACT

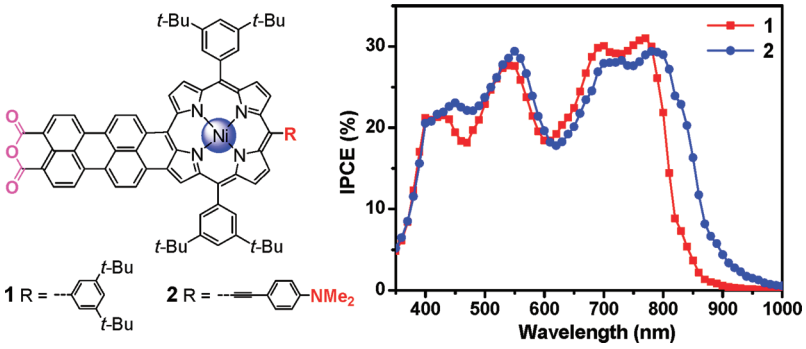

Two perylene anhydride fused porphyrins 1 and 2 have been synthesized and employed successfully in dye-sensitized solar cells (DSCs). Both compounds showed broad incident monochromatic photon-to-current conversion efficiency spectra covering the entire visible spectral region and even extending into the near-infrared (NIR) region up to 1000 nm, which is impressive for ruthenium-free dyes in DSCs.

Recent developments in the field of organic solar cells have boosted interest in development of novel functional near-infrared (NIR) dyes,[1] given that sunlight possesses 50% of its irradiation energy in the infrared spectral region. Dye-sensitized solar cells (DSCs)[2] stand out to challenge the traditional silicon-based solar cells due to the cost-effectiveness issue combined with their medium efficiencies. A rising interest is to use ruthenium-free dyes as sensitizers for DSCs,[3,4] because such dyes hold many advantages over ruthenium-based dyes such as lower cost, higher absorption coefficient, and ease of tuning LUMO and HOMO energy levels. However, how to obtain a single sensitizer that is capable of effectively capturing light over the entire spectrum from 400 to 1000 nm and simultaneously fulfills all the requirements for an efficient device remains a long-term challenge.[5]

[†] National University of Singapore.
[‡] Changchun Institute of Applied Chemistry.
[§] King Abdullah University of Science and Technology.
[∥] Institute of Materials Research and Engineering.

(1) For selected reviews, see: (a) Fabian, J.; Nakanzumi, H.; Matsuoka, M. *Chem. Rev.* **1992**, *92*, 1197–1226. (b) Qian, G.; Wang, Z. *Chem. Asian J.* **2010**, *5*, 1006–1029. (c) Jiao, C.; Wu, J. *Curr. Org. Chem.* **2010**, *14*, 2145–2168.

(2) (a) O'Regan, B.; Grätzel, M. *Nature* **1991**, *353*, 737–740. (b) Hagfeldt, A.; Grätzel, M. *Chem. Rev.* **1995**, *95*, 49–68.

(3) For recent reviews, see: (a) Mishra, A.; Fischer, M. K. R.; Bäuerle, P. *Angew. Chem., Int. Ed.* **2009**, *48*, 2474–2499. (b) Li, C.; Liu, M.; Pschirer, N. G.; Baumgaten, M.; Müllen, K. *Chem. Rev.* **2010**, *110*, 6817–6855. (c) Hagfeldt, A.; Boschloo, G.; Sun, L.; Kloo, L.; Pettersson, H. *Chem. Rev.* **2010**, *110*, 6595–6663.

(4) For refernces concerning high-efficiency DSCs, see: (a) Zeng, W.; Cao, Y.; Bai, Y.; Wang, Y.; Shi, Y.; Zhang, M.; Wang, F.; Pan, C.; Wang, P. *Chem. Mater.* **2010**, *22*, 1915–1925. (b) Bessho, T.; Zakeeruddin, S. M.; Yeh, C.-Y.; Diau, E. W.-G.; Grätzel, M. *Angew. Chem., Int. Ed.* **2010**, *49*, 6646–6649.

(5) Yum, J. H.; Baranoff, E.; Wenger, S.; Nazeeruddin, M. K.; Grätzel, M. *Energy Environ. Sci.* **2011**, *4*, 842–857.

10.1021/ol201303h
Published on Web 06/23/2011

Porphyrin has gained recognition as one of the most versatile building blocks for DSCs due to their unique optical as well as electrochemical properties and their excellent photochemical stability.[6] Due to the limited absorption behavior of the porphyrin monomer in the visible and particularly in the NIR region, efforts have been made toward the design and synthesis of π-extended porphyrins, including porphyrin tapes[7] and polycyclic aromatic compounds-fused porphyrins,[8] which were predicted to have potential applications in photovoltaic devices.[8e,h,i] Attempts to use these fused dyes in DSCs were independently made by Yeh and Imahori's groups,[9,10] and up to 4.1% efficiency was achievable under optimized conditions. However, DSCs based on fused porphyrin systems exhibiting a NIR response beyond 900 nm have never been reported. Herein we report two novel perylene anhydride fused porphyrin dyes **1** and **2** (Figure 1), which have been employed successfully as NIR sensitizers for DSCs.

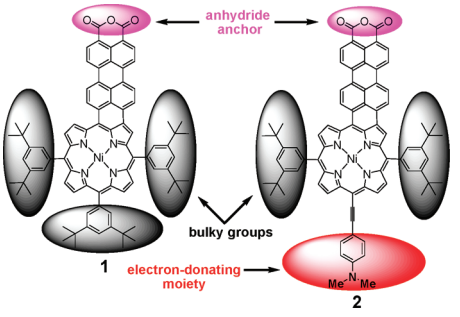

Figure 1. Molecular design and structures of dyes **1** and **2**.

As shown in Figure 1, the molecular design is based on the following considerations: (1) Perylene monoimide-fused porphyrins exhibit intensified NIR absorptions, large dipole moments, and high photostability as reported in our recent studies,[8h] thus providing an extraordinary molecular platform for applications in DSCs. Nevertheless, appropriate structural modifications are necessary for such a purpose. (2) Anhydride serves as an anchoring group,[11] which can be obtained by saponification of an imide group in the presence of a strong base. In addition, the electron-withdrawing anhydride moiety is able to stabilize the highly conjugated low band gap π-system,[8h] leading to stable NIR dyes for practical DSCs application. (3) In the design of the large-sized, rigid molecules **1** and **2**, bulky 3,5-di-*tert*-butylphenyl groups were chosen as substituents because such bulky groups not only surmount the solubility problem but also eliminate the aggregation of the chromophores.[8e−g] (4) Introduction of an electron-donating 4-(dimethylamino)-phenylethynylene onto the *meso*-position of porphyrin in **2** is supposed to result in a more red-shifted NIR absorption due to the enhanced intramolecular charge transfer, and this is also beneficial to a fast electron injection from the excited dye to the conduction band of TiO_2 in DSCs.[3c]

Scheme 1

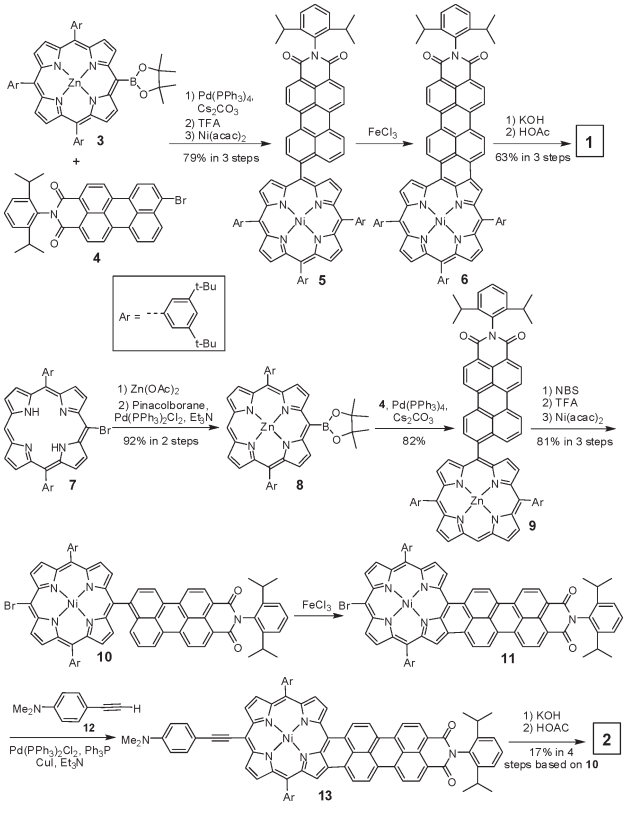

(6) For selected reviews, see: (a) Imahori, H.; Umeyama, T.; Ito, S. *Acc. Chem. Res.* **2009**, *42*, 1809–1818. (b) Martínez-Díaz, M. V.; de la Torre, G.; Torres, T. *Chem. Commun.* **2010**, *46*, 7090–7108. (c) Radivojevic, I.; Varotto, A.; Farleya, C.; Drain, C. M. *Energy Environ. Sci.* **2011**, *3*, 1897–1909.

(7) (a) Tsuda, A.; Osuka, A. *Science* **2001**, *293*, 79–82. (b) Ikda, T.; Aratani, N.; Osuka, A. *Chem. Asian J.* **2009**, *4*, 1248–1256.

(8) For selected references, see: (a) Gill, H. S.; Marmjanz, M.; Santamaría, J.; Finger, I.; Scott, M. J. *Angew. Chem., Int. Ed.* **2004**, *43*, 485–490. (b) Yamane, O.; Sugiura, K.; Miyasaka, H.; Nakamura, K.; Fujimoto, T.; Nakamura, K.; Kaneda, T.; Sakata, Y.; Yamashita, M. *Chem. Lett.* **2004**, *33*, 40–41. (c) Kurotobi, K.; Kim, K. S.; Noh, S. B.; Kim, D.; Osuka, A. *Angew. Chem., Int. Ed.* **2006**, *45*, 3944–3947. (d) Tokuji, S.; Takahashi, Y.; Shinmori, H.; Shinokubo, H.; Osuka, A. *Chem. Commun.* **2009**, 1028–1030. (e) Davis, N. K. S.; Thompson, A. L.; Anderson, H. L. *Org. Lett.* **2010**, *12*, 2124–2127. (f) Diev, V. V.; Hanson, K.; Zimmerman, J. D.; Forrest, S. R.; Thompson, M. E. *Angew. Chem., Int. Ed.* **2010**, *49*, 5523–5526. (g) Jiao, C.; Huang, K.-W.; Guan, Z.; Xu, Q.-H.; Wu, J. *Org. Lett.* **2010**, *12*, 4046–4049. (h) Jiao, C.; Huang, K.-W.; Chi, C.; Wu, J. *J. Org. Chem.* **2011**, *76*, 661–664. (i) Davis, N. K. S.; Thompson, A. L.; Anderson, H. L. *J. Am. Chem. Soc.* **2011**, *133*, 30–31. (j) Jiao, C.; Zhu, L.; Wu, J. *Chem.—Eur. J.* **2011**, *17*, 6610–6614.

(9) Mai, C.-L.; Huang, W.-K.; Lu, H.-P.; Lee, C.-W.; Chiu, C.-L.; Liang, Y.-R; Diau, E. W.-G.; Yeh, C.-Y. *Chem. Commun.* **2010**, *46*, 809–811.

(10) (a) Tanaka, M.; Hayashi, S.; Eu, S.; Umeyama, T.; Matano, Y.; Imahori, H. *Chem. Commun.* **2007**, 2069–2071. (b) Hayashi, S.; Tanaka, M.; Hayashi, H.; Eu, S.; Umeyama, T.; Matano, Y.; Araki, Y.; Imahori, H. *J. Phys. Chem. C* **2008**, *112*, 15576–15585.

(11) (a) Edvinsson, T.; Li, C.; Pschirer, N.; Schöneboom, J.; Eickemeyer, F.; Sens, R.; Boschloo, G.; Herrmann, A.; Müllen, K.; Hagfeldt, A. *J. Phys. Chem. C* **2007**, *111*, 15137–15140. (b) Li, C.; Yum, J.-H.; Moon, S.-J.; Herrmann, A.; Eickemeyer, F.; Pschirer, N. G.; Erk, P.; Schöneboom, J.; Müllen, K.; Grätzel, M.; Nazeeruddin, M. K. *ChemSusChem.* **2008**, *1*, 615–618. (c) Li, C.; Liu, Z.; Schöneboom, J.; Eickemeyer, F.; Pschirer, N. G.; Erk, P.; Herrmann, A.; Müllen, K. *J. Mater. Chem.* **2009**, *19*, 5405–5415.

Scheme 1 outlines the synthetic route for compounds **1** and **2** (see Supporting Information for more details). The synthesis commenced with the preparation of the precursor **5**, which was synthesized by Suzuki coupling of porphyrin boronic ester **3**[12] and perylene monoimide **4**[13] followed by demetalation and Ni(II)-metalation. Intramolecular cyclization reaction of **5** promoted by $FeCl_3$ then generated a purple solid as a mixture containing unseparable chlorinated side products, which was directly converted to their corresponding anhydrides without purification. Separation of **1** from other side products was successful after saponification of **6** with an overall yield of 63% for three steps based on **5**. Preparation of electron-donating 4-(dimethylamino)phenylethynylene substituted **2** followed a slightly revised procedure. The key intermediate **10** was first prepared by sequential Miyaura reaction, Suzuki coupling, bromination, and trans-metalation. In common with the synthesis of **6**, $FeCl_3$-promoted oxidative dehydrogenation of **10** afforded fused **11** together with some chlorinated side products. The presence of bromine atom in **11** allowed further functionalization, and the incorporation of an electron-donating 4-(dimethylamino)phenylethynylene group was carried out at this stage by Sonogashira–Hagihara coupling reaction to generate "push-pull" type molecule **13**, which finally underwent saponification to give target molecule **2** with an overall yield of 17% for four steps based on **10**.

The absorption spectra of both **1** and **2** cover the entire visible and a part of the NIR spectral region (Figure 2). The absorption maximum of **1** was found at 805 nm

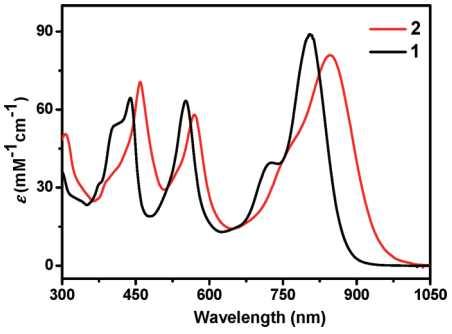

Figure 2. UV–vis–NIR absorption spectra of **1** and **2** in $CHCl_3$ (8.0×10^{-6} M).

(ε = 89,000 M^{-1} cm^{-1}), and a further red-shift of 42 nm was observed for **2** (ε = 81,000 M^{-1} cm^{-1}) owing to enhanced intramolecular charge transfer. Nearly no fluorescence was observed for **1** and **2** in chloroform, which is common for Ni(II)-porphyrins. In addition, other factors such as aggregation and photoinduced intramolecular charge transfer from porphyrin to perylene anhydride can also decrease the fluorescence quantum yield.

Electrochemical properties of **1** and **2** were investigated by cyclic voltammetry in deoxygenated DCM solution containing 0.1 M tetra-*n*-butylammonium hexafluorophosphate as supporting electrolyte (Table S1 and Figure S1 in Supporting Information). Compound **1** exhibited four reversible oxidation waves with half-wave potentials at 0.29, 0.45, 0.73, and 0.83 V (versus Fc^+/Fc), whereas three reversible or quasireversible oxidative waves were observed with half-wave potentials potentials at 0.15, 0.25, and 1.02 V for **2**; these are distinguishable by differential-pulse voltammetry (DPV). Furthermore, two reversible reduction waves were found for both **1** and **2** with half-wave potentials at −0.94 and −1.04 V for **1** and at −0.94 and −1.05 V for **2**, indicating that they can be reduced into the corresponding radical anions and dianions, which can also be stabilized by the delocalized π-system. HOMO energy levels of −5.04 and −4.89 eV and LUMO energy levels of −3.92 and −3.93 eV were estimated for **1** and **2**, respectively.[14] Energy gaps of 1.12 eV for **1** and 0.94 eV for **2** were then calculated, and this trend is in agreement with their optical band gaps (1.42 eV for **1** and 1.31 eV for **2**).

To gain better insight into the molecular geometries, molecular orbitals, and UV–vis–NIR absorption spectra of **1** and **2**, time-dependent density function theory (TDDFT at B3LYP/6-31G**) calculations were performed, and the optimized molecular structures and frontier molecular orbital profiles are shown in Figure 3. The HOMO for both **1** and **2** are delocalized throughout the

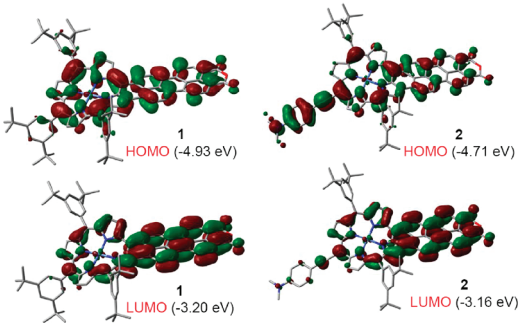

Figure 3. Frontier molecular orbital profiles of molecules **1** and **2** calculated by DFT.

highly conjugated backbone as well as the terminal amino group. In contrast, the LUMO for **1** and **2** are predominately located at the perylene anhydride motif. Such orbital partitions are undoubtedly beneficial for electron injection and overall photovoltaic performance. The calculations also predict that **1** and **2** will show absorption maximum at 759 and 849 nm (Figures S2, S3 and Tables

(12) (a) Wang, Q. M.; Bruce, D. W. *Synlett* **1995**, 1267–1268. (b) Nakamura, Y.; Jang, S. Y.; Tanaka, T.; Aratani, N; Lim, J. M.; Kim, K. S.; Kim, D.; Osuka, A. *Chem.—Eur. J.* **2008**, *14*, 8279–8289.

(13) Baffreau, J.; Ordronneau, L.; Leroy-Lhez, S.; Hudhomme, P. *J. Org. Chem.* **2008**, *73*, 6142–6147.

(14) The HOMO and LUMO energy levels were calculated from the onset of the first oxidation and reduction waves according to the following equations: HOMO = $-(4.8 + E_{ox}^{onset})$ and LUMO = $-(4.8 + E_{red}^{onset})$.

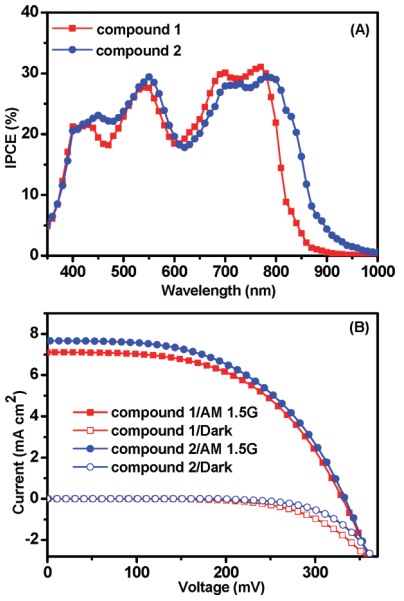

Figure 4. (A) IPCE spectra of the devices sensitized by **1** and **2**. (B) $J-V$ curves of DSCs based on **1** and **2** at an irradiation of 100 mW cm^{-2} AM 1.5 G sunlight.[16]

S2–S5 in Supporting Information), respectively, which are in good agreement with the experimental data.

The DSC devices applying **1** and **2** as NIR sensitizers were constructed and characterized (see Supporting Information for experimental details). As shown in Figure 4A, the preliminary investigation of the incident monochromatic photon-to-current conversion efficiency (IPCE) revealed that IPCE spectra reached the highest values of 31.4% at 772 nm for **1** and 29.7% at 790 nm for **2**, respectively. In common with their absorption spectra, IPCE curves for both **1** and **2** not only exhibit panchromatic responses but also extend the photovoltaic performance to the NIR region. Noteworthy is that dye **2** displays an IPCE response as long as 1000 nm, which is one of the furthest red-shifted responses reported for ruthenium-free DSCs. The characteristic current density–voltage ($J-V$) curve measured under irradiation of AM 1.5 G full sunlight (Figure 4B) provides a short-circuit current density (J_{sc}) of 7.11 mA/cm^2, an open-circuit voltage (V_{oc}) of 329 mV, and a fill factor (FF) of 0.54, yielding the overall power conversion efficiency (η) of 1.26% for a DSC device based on **1**. For comparison, photovoltaic parameters (J_{sc}, V_{oc}, FF, and η) of **2** are 7.66 mA/cm^2, 333 mV, 0.52, and 1.36%, respectively. The results demonstrate that the attachment of electron-donating amino groups onto the π-conjugation system for **2** slightly increases the J_{sc} but has no positive effect on V_{oc} and FF. The moderate efficiencies of NIR dyes **1** and **2** perhaps are attributed to the following reasons: (1) The LUMO energy levels of **1** and **2** are very close to the conduction band edge of TiO_2, thus leading to insufficient driving force for electron injection.[9] (2) Depite the introduction of bulky groups, dyes **1** and **2** still have a strong tendency to form aggregates, reflected by their broad ^{1}H NMR spectra recorded at room temperature. It is commonly believed that aggregation of dyes reults in nonradiative decay of dyes from the excited state to the ground state. Excitons, therefore, are readily trapped or quenched by aggregate states, which eventually reduces photocurrent densities.[3] (3) The short lifetime of the excited states of the dyes possibly decreases the device performance, because short lifetime narrows the time-scale window when electron injection takes place.[15]

In summary, a new strategy for designing NIR dyes for DSCs by fusing an electron-rich porphyrin unit to the perylene anhydride core was demonstrated. Based on dyes **1** and **2**, broader IPCE spectra have been achieved, covering the entire visible range extending into the NIR region up to 1000 nm. Although these NIR dyes displayed moderate efficiencies, the enhanced light harvesting properties in the NIR region provide possibilities for further improvement of overall DSC efficiency of ruthenium-free sensitizers with panchromatic and particularly NIR response. Further structural optimization, such as reducing the aggregation and tuning the energy levels, is very likely to generate more efficient sensitizers and this work is currently underway in our laboratories.

Acknowledgment. J.W. acknowledges financial support from Singapore DSTA DIRP Project (DSTA-NUS-DIRP/2008/03), NRF Competitive Research Program (R-143-000-360-281), NUS Young Investigator Award (R-143-000-356-101), A*Star BMRC-NMRC joint grant (no. 10/1/21/19/642), and IMRE Core Funding (IMRE/10-1P0509). K.-W.H. acknowledges the financial support from KAUST.

Supporting Information Available. Experimental details, characterization data of all new compounds, theoretical calculation data, CV data, and the detailed device fabrication as well as the photovoltaic characterizations. This material is available free of charge via the Internet at http://pubs.acs.org.

(15) (a) Cherepy, N. J.; Smestad, G. P.; Grätzel, M.; Zhang, J. Z. *J. Phys. Chem. B* **1997**, *101*, 9342–9351. (b) Kira, A; Matsubara, Y.; Iijima, H.; Umeyama, T.; Matano, Y.; Ito, S.; Niemi, M.; Tkachenko, N. V.; Lemmetyinen, H.; Imahori, H. *J. Phys. Chem. C* **2010**, *114*, 11293–11304.

(16) The spectral distribution of our light resource simulates AM 1.5 G solar emission with a mismatch less than 5%.